united nations
educational, scientific
and cultural
organization

international atomic
energy agency

the
abdus salam
international centre for theoretical physics

Winter College on Optics and Photonics
7 - 25 February 2000

1218-16

"Low Dimensional Semiconductor LASER"

L. SORBA
Laboratorio TASC-INFM, Trieste
Italy
and
Univ. di Modena e Reggio Emilia, Modena
Italy

INFM

Low Dimensional Semiconductor LASER

Lucia Sorba
Laboratorio TASC-INFM, Trieste (Italy) and
Universita'di Modena e Reggio Emilia, Modena (Italy)

Today

- Wide gap materials for blue-green optoelectronic applications
- AlGaAs/GaAs T-shaped Quantum Wire LASERS

Motivation

Enormous technological impact of wide gap LASER for large device applications: optical communications, CD players etc.

II-VI

II-VI/III-V heterojunctions are crucial elements for II-VI blue-green LASERS.

Native stacking faults control the LASER degradation.

GaN-AlGaN

Very high efficency.

Lack of substrates: SiC(3.5%), Sapphire (14%).

Large number of threading dislocations ($1\text{x}10^8$ to $1\text{x}10^{12}$ cm^{-2}).

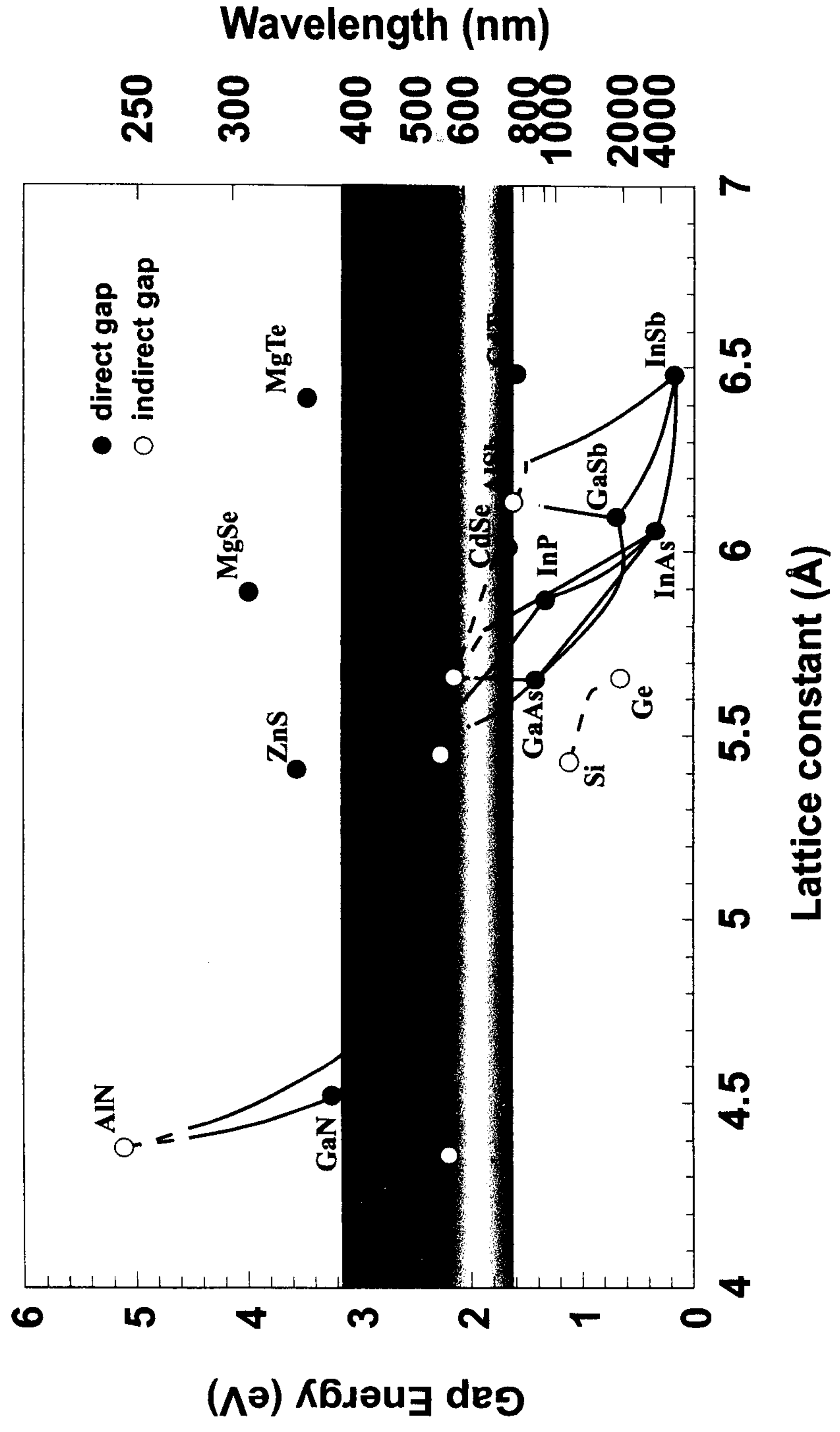
Wavelength (nm)
250
300
400
500
600
800
1000
2000
4000
Gap Energy (eV)
0
1
2
3
4
5
6
Lattice constant (Å)
4
4.5
5
5.5
6
6.5
7
● direct gap
○ indirect gap
AlN
GaN
ZnS
MgSe
MgTe
CdSe
GaAs
InP
Si
Ge
GaSb
InAs
InSb

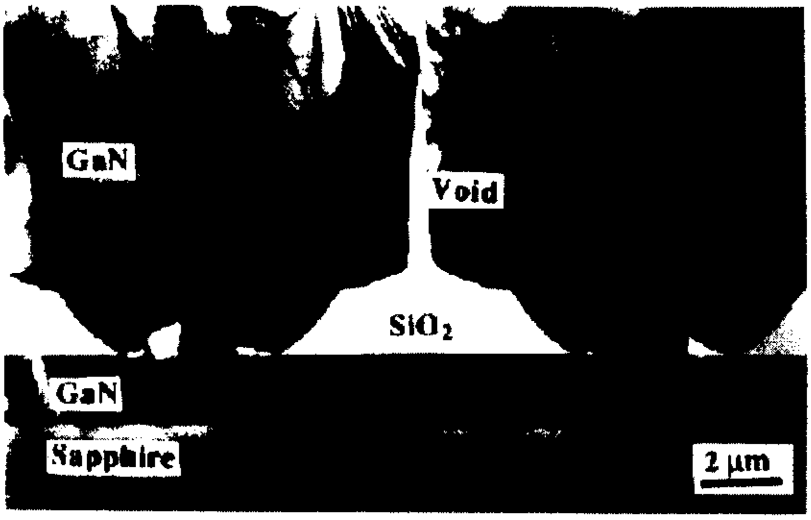

Fig. 5. Cross-sectional TEM micrograph of the laterally overgrown GaN layer on a SiO$_2$ mask and window area.

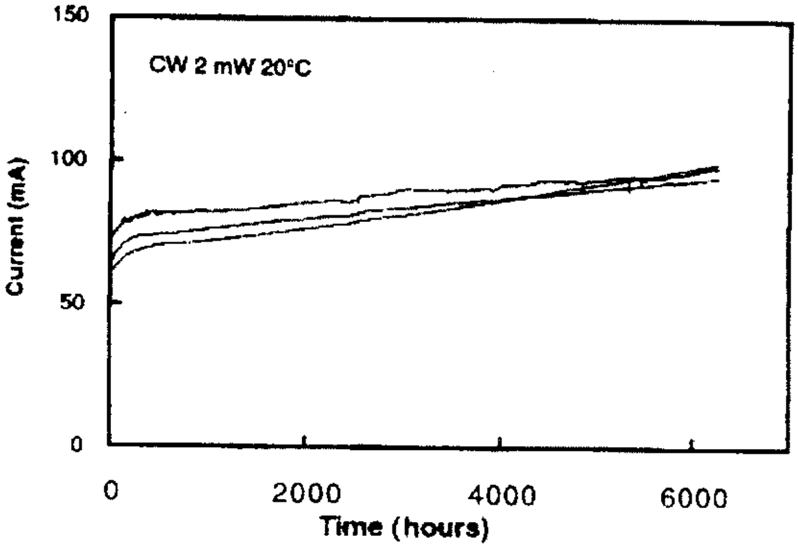

Fig. 6. Operating current as a function of time under a constant output power of 2 mW per facet controlled with an autopower controller. The LDs with MD-SLS cladding layers grown on the ELOC substrate were operated under dc at RT.

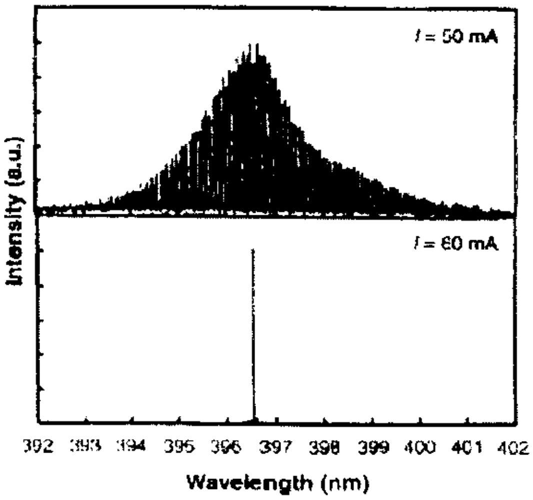

Fig. 7. Laser emission spectra measured under RT CW operation wi currents of 50 and 60 mA.

Nakamura, Science **281** (1998), 956

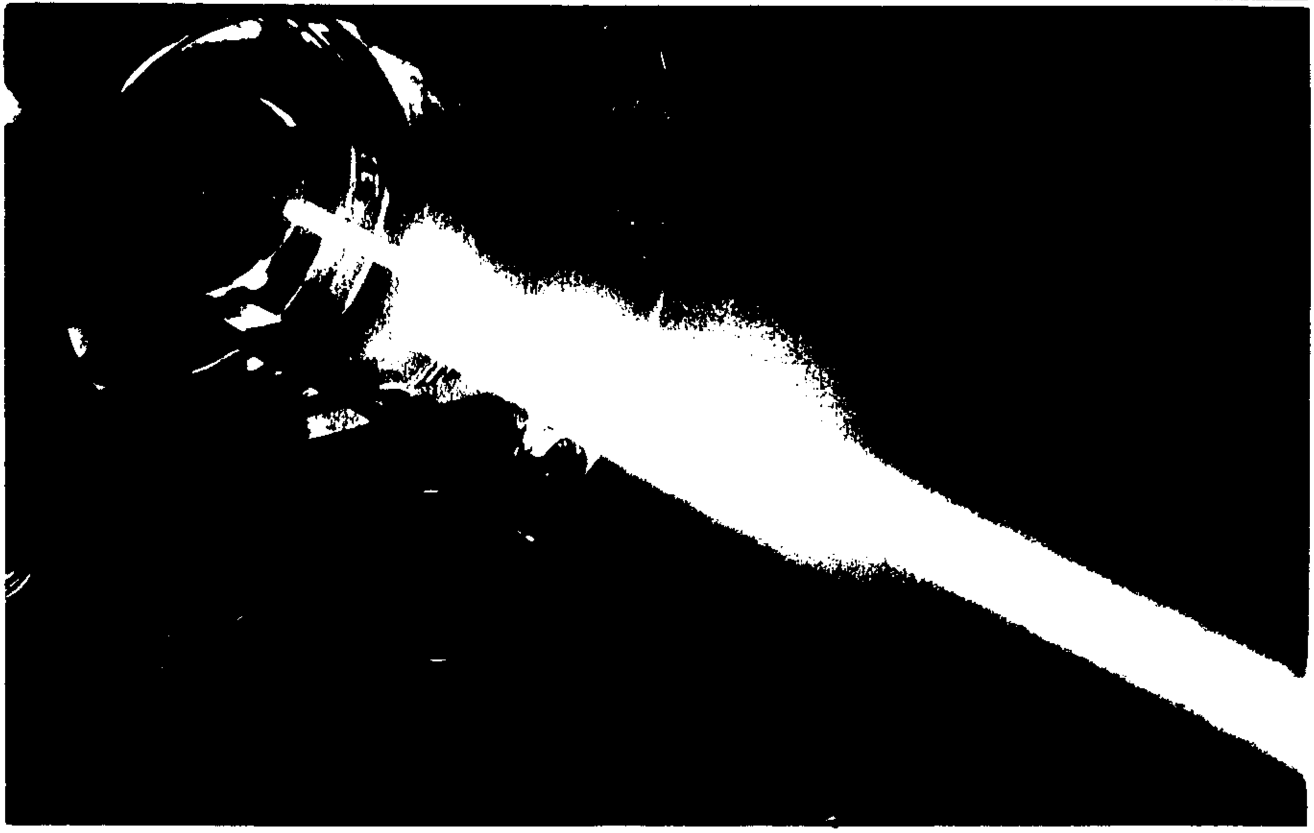

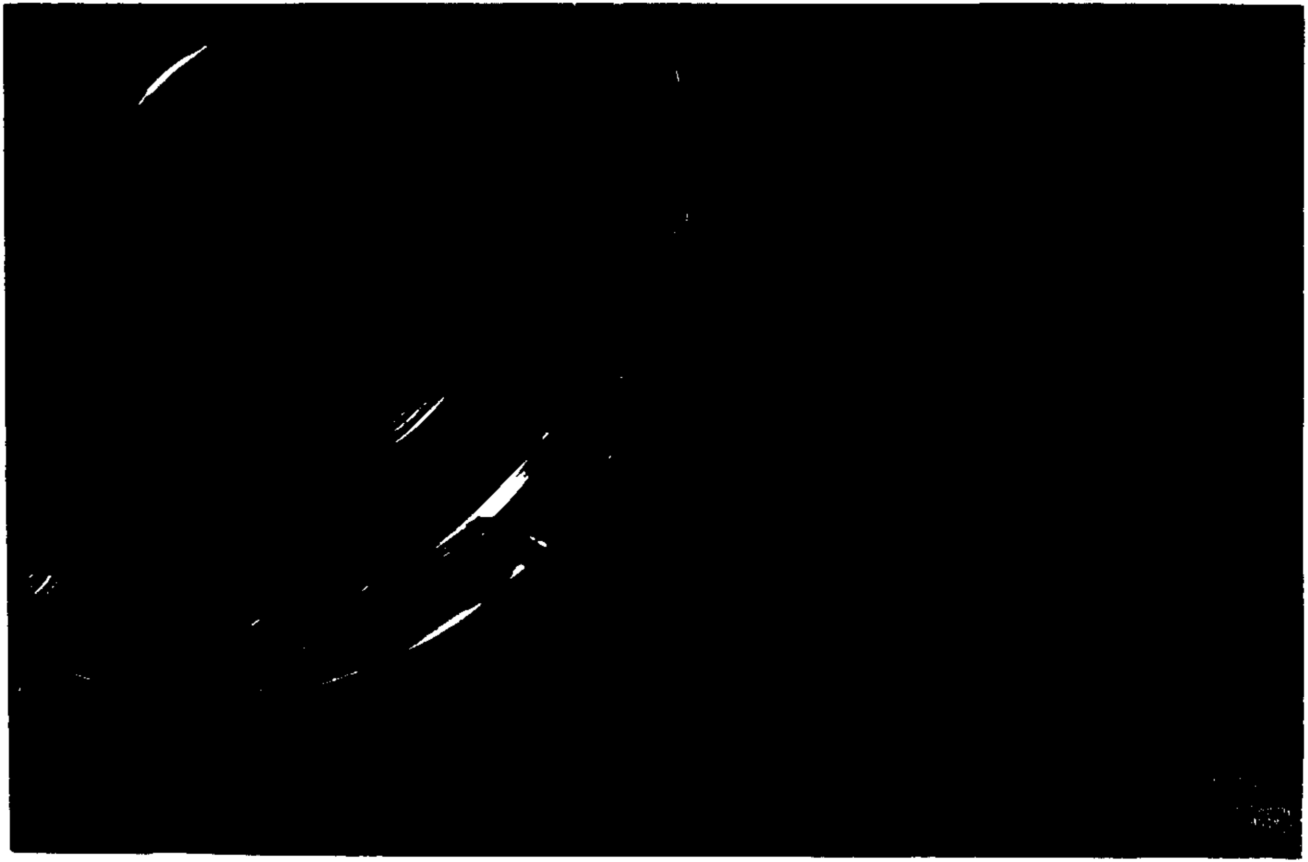

3M

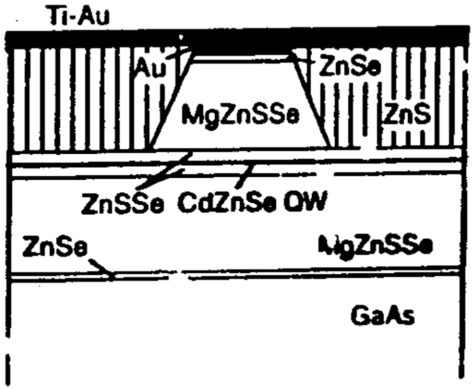

Sony

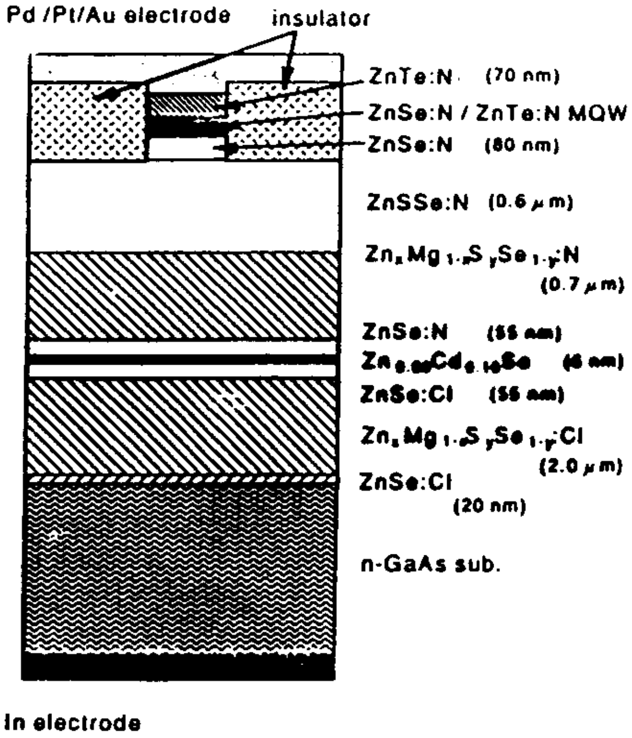

M.A. Haase et al., Appl. Phys. Lett. **63**, 2315 (1993)
S. Itoh et al., Jpn. J. Appl. Phys. **32**, L1530 (1993)
N. Nakayama et. al., Elett. Letters 29, 2194 (1993)

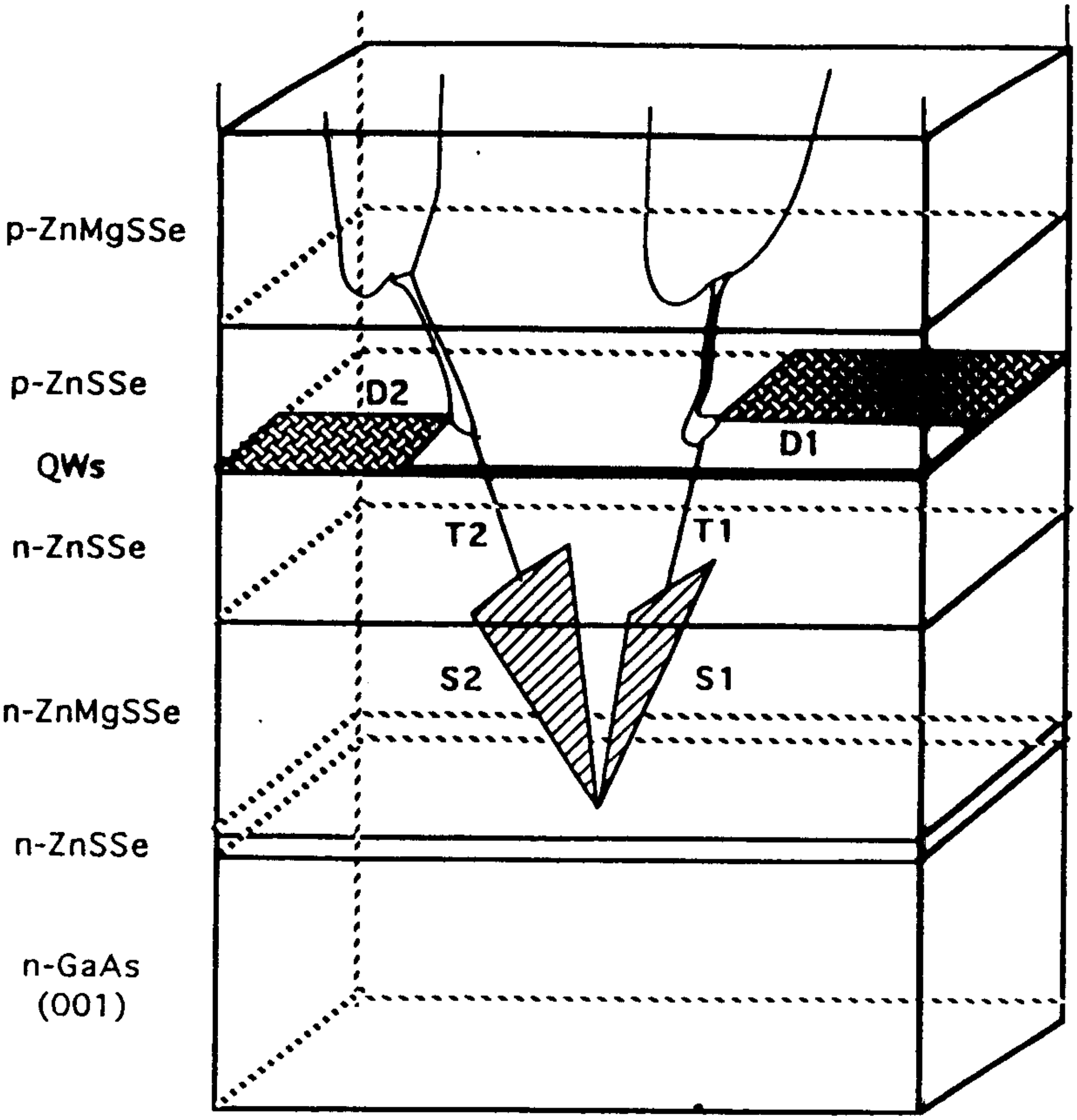

FIG. 3. Schematic showing the three dimensional arrangement of the defects shown in Fig. 2.

Table I

Density of Faulted Defects in ZnS_xSe_{1-x} as a Function of Growth Conditions

Growth mode	GaAs Surface	Surface Treatment	Density of Frank Partial Dislocations	Density of Schockley Partial Dislocations
2-D within 20 secs	Ga-stabilized	None	$1 \times 10^8/cm^2$	$7 \times 10^7/cm^2$
2-D within 8-9 secs	As-stabilized	Se	$2 \times 10^8/cm^2$	$5 \times 10^7/cm^2$
2-D within 8-9 secs	As-terminated	Zn	$1 \times 10^6/cm^2$	$2 \times 10^8/cm^2$
2-D right away	As-stabilized	None	$1 \times 10^7/cm^2$	$1 \times 10^6/cm^2$
2-D right away	As-rich	Zn	$5 \times 10^7/cm^2$	< [illegible] $\times 10^4/cm^2$

[redacted]

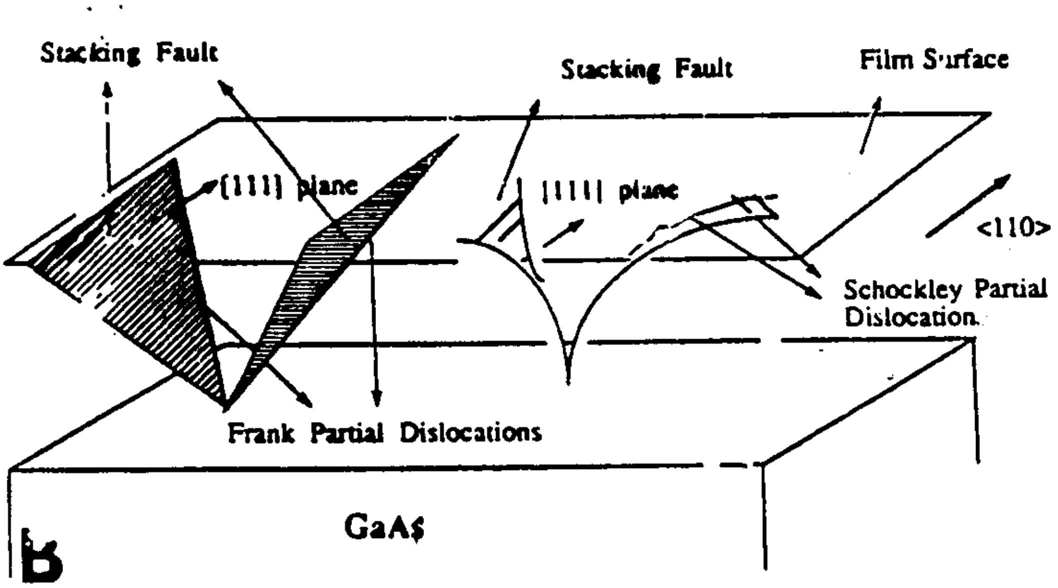

L.K Kuo et al., Spie proc. Vol. 2346, 147 (1994)

Appl. Phys. Lett. 65 (1994) 1230

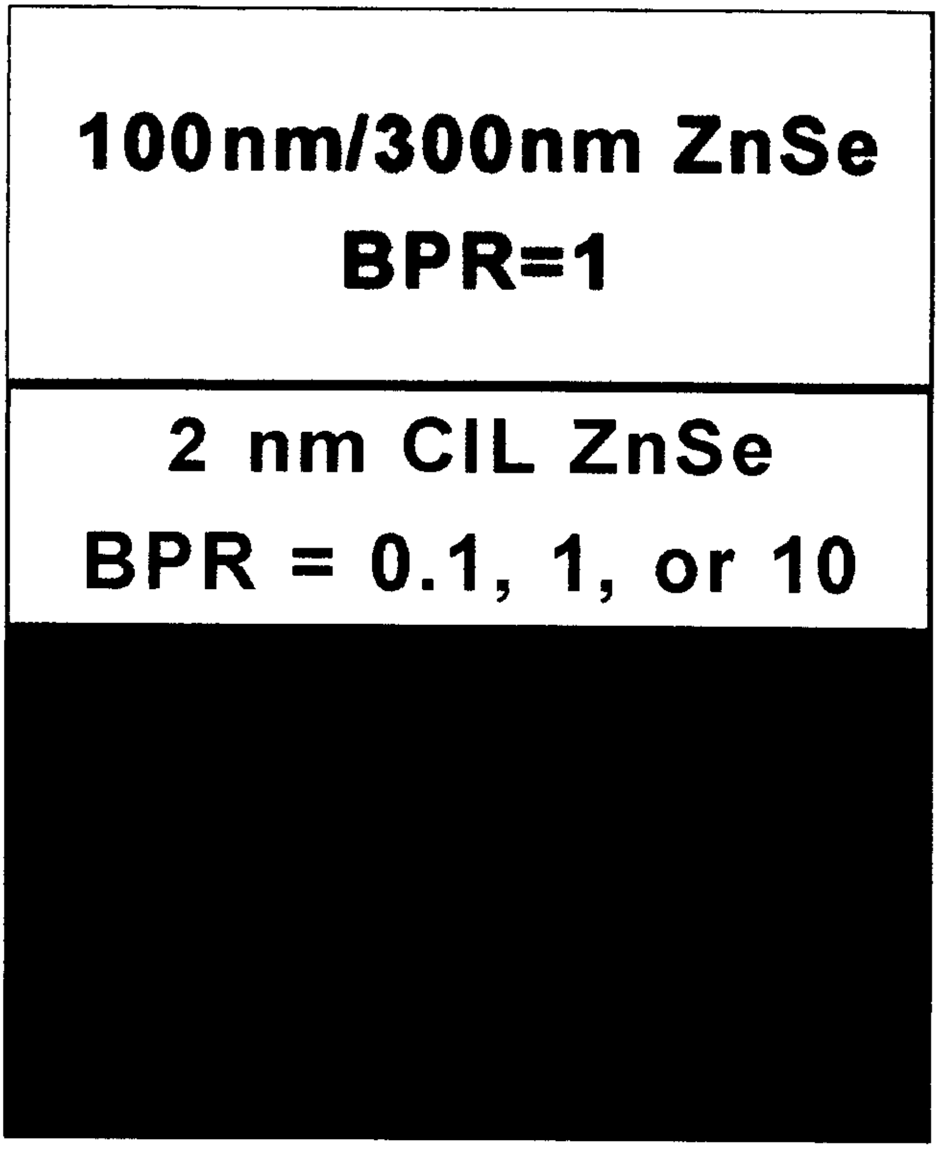
100nm/300nm ZnSe
BPR=1
2 nm CIL ZnSe
BPR = 0.1, 1, or 10

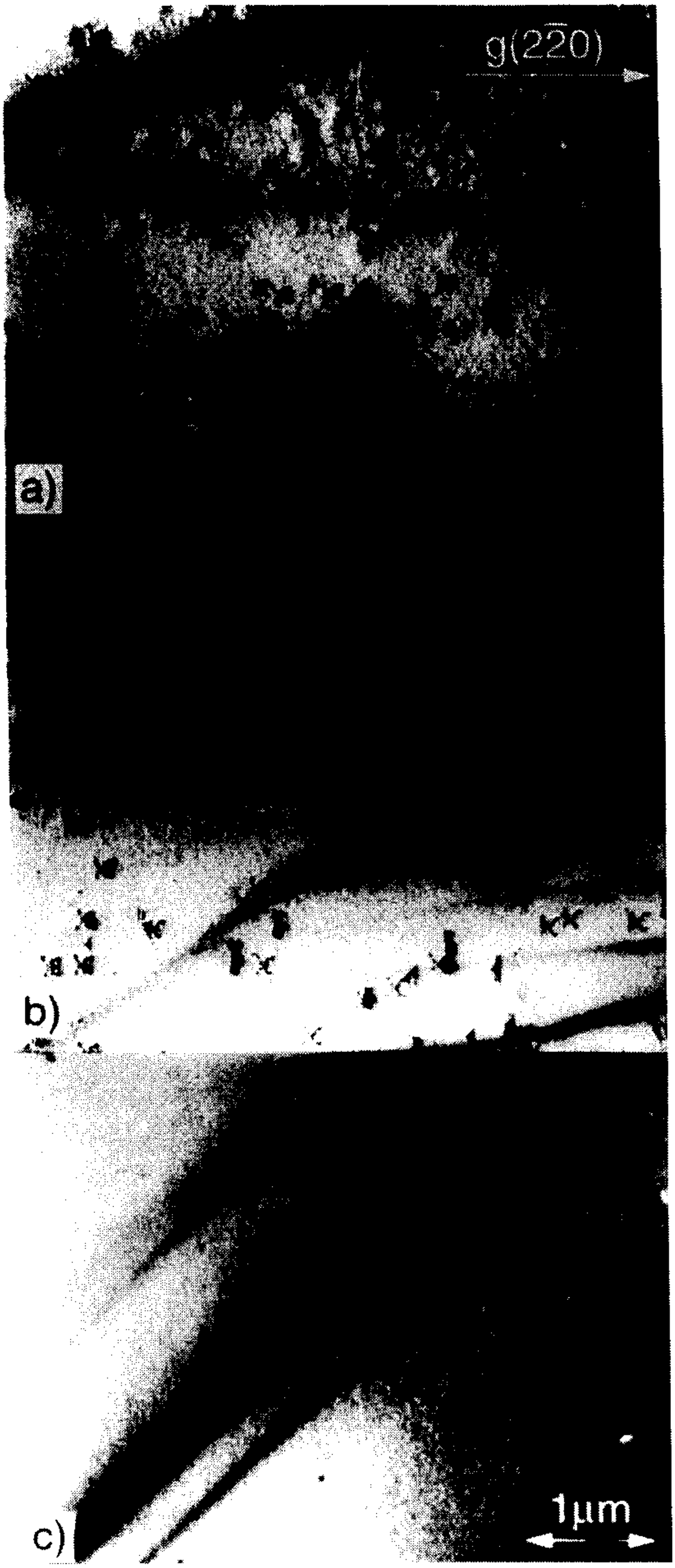

EPR = 10

[illegible]

EPR = 1

[illegible]

EPR = 0.1

[illegible]

S. Hain et al. APL 70, 237 (1997)
S. Hain et al. J.V.S.T. B15, 1279 (1997)

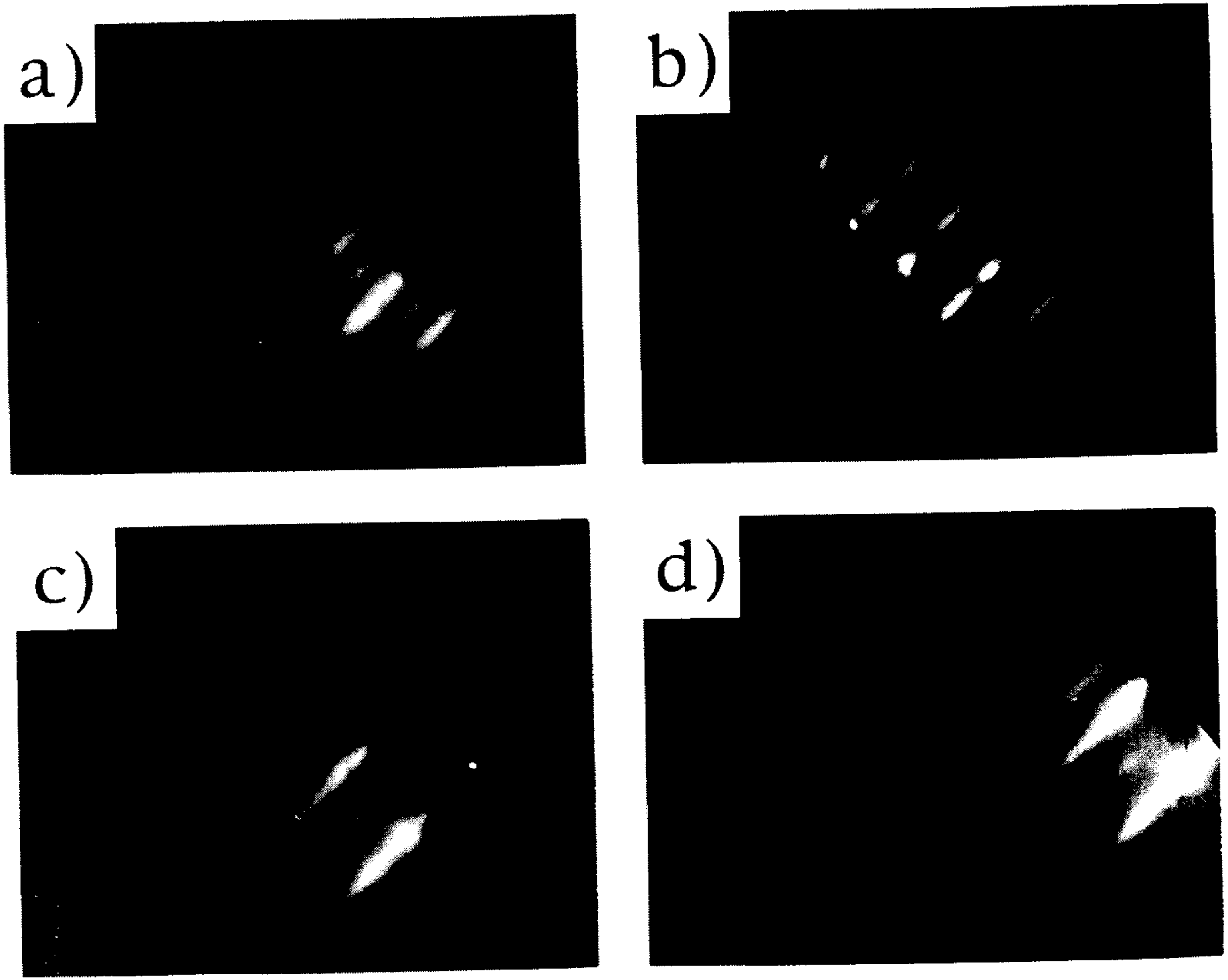

2 nm ZnSe / GaAs (001)

[001]
ZnAs??

Zn-ri

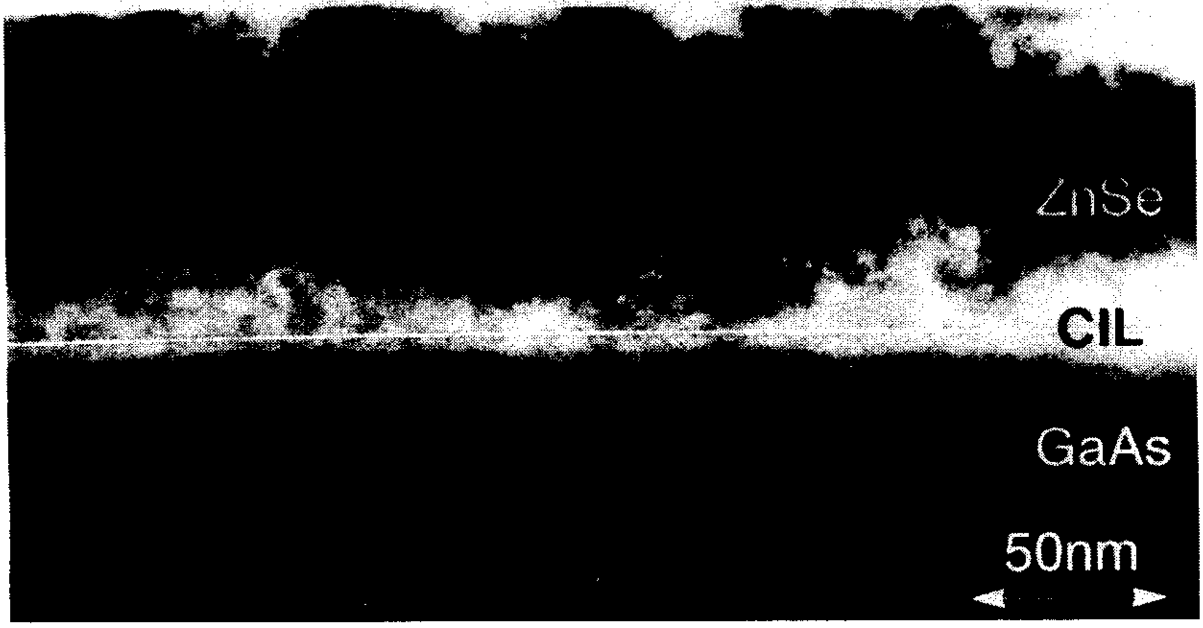

Se-ri

Conclusions:

Schockley stacking fault (SF) pairs most common defects

Se-rich interfaces yield 3-4 orders of magnitude lower densities of Schockley SF pairs than Zn-rich interfaces

Isolated Frank SF also affected but to lesser extent

-> Interface composition controls the SF density

2D growth for both Se-rich and Zn-rich interfaces

Lateral inhomogeneities observed for Zn-rich interfaces

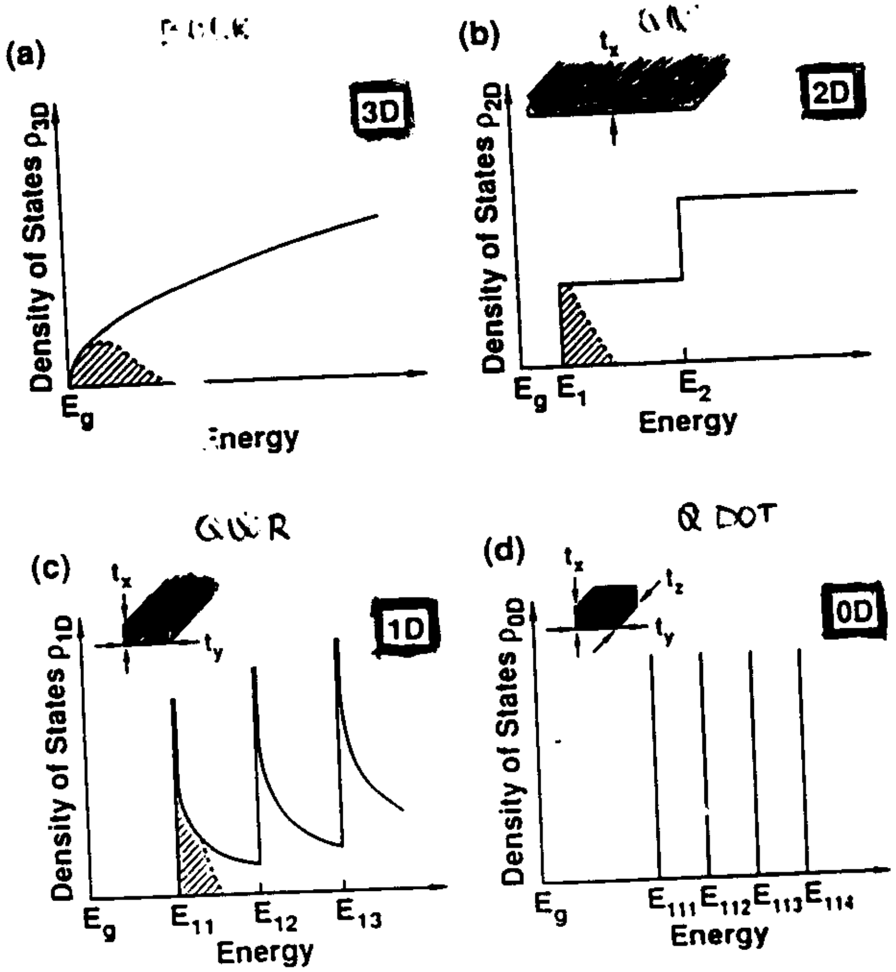

Fig. 1. Schematic description of the density of states versus dimensionality. The insets illustrate rectangular potential well configurations of the corresponding quantum-confined structure. (a) Bulk (3D); (b) quantum well (2D); (c) quantum wire (1D); (d) quantum dot (0D). The crossed areas indicate occupied states for similar carrier density. (after [87], © 1992 IEEE.)

INFM QWR LASER

Sharp peaks in the density of states of lower dimensional systems (1D and 0D) should lead to interesting improved laser performance

- Narrower optical gain spectra

- Higher differential gain

- Lower threshold current and reduced temperature sensitivity

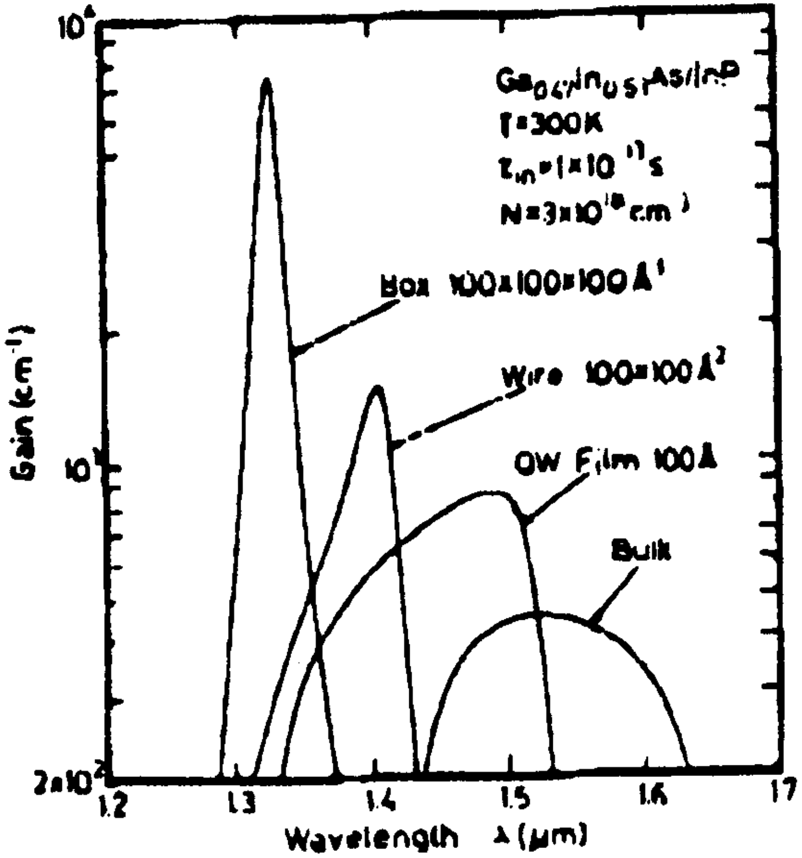

QWR LASER

Reduction of dimensionality was achieved by application of B // to the growth direction in MQW LASERS:

- Improved LASER characteristics
- Increased threshold current and unaffected intensity emission

Operation of AlGaAs/GaAs QWR LASER with I_{th}=0.4mA at 4.2K (W. Wegscheider et al. APL 65, 2510 (1996)).

Investigation of dynamical properties of QWR LASER (W. Wegscheider et al. Solid State Electr. 40, 4 (1996))

INFM Cleaved Edge Overgrowth Method

Fabrication process characteristics of CEO*

- MBE technique

- High-quality regrowth on the cleaved edge of multilayer sample

- Perfect structures with atomic control in two dimensions
  (T-shaped wires, dots)

- Size, shape and positions

*L. Pfeiffer et al. APL **56**, (1990) 1697

INFM Optically pumped LASER

LASER structure

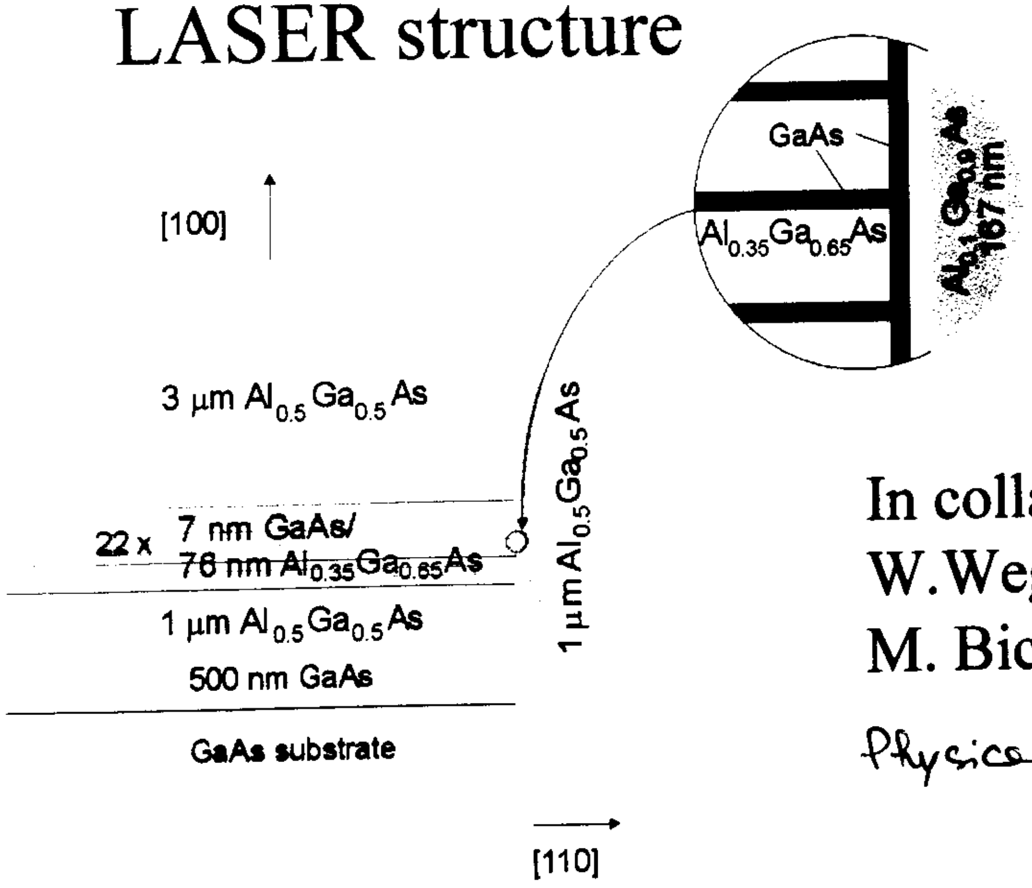

In collaboration with
W.Wegscheider, G. Schedelbeck,
M. Bichler, and G. Abstreiter,
Physica Status Solidi in press

INFM Output Characteristics

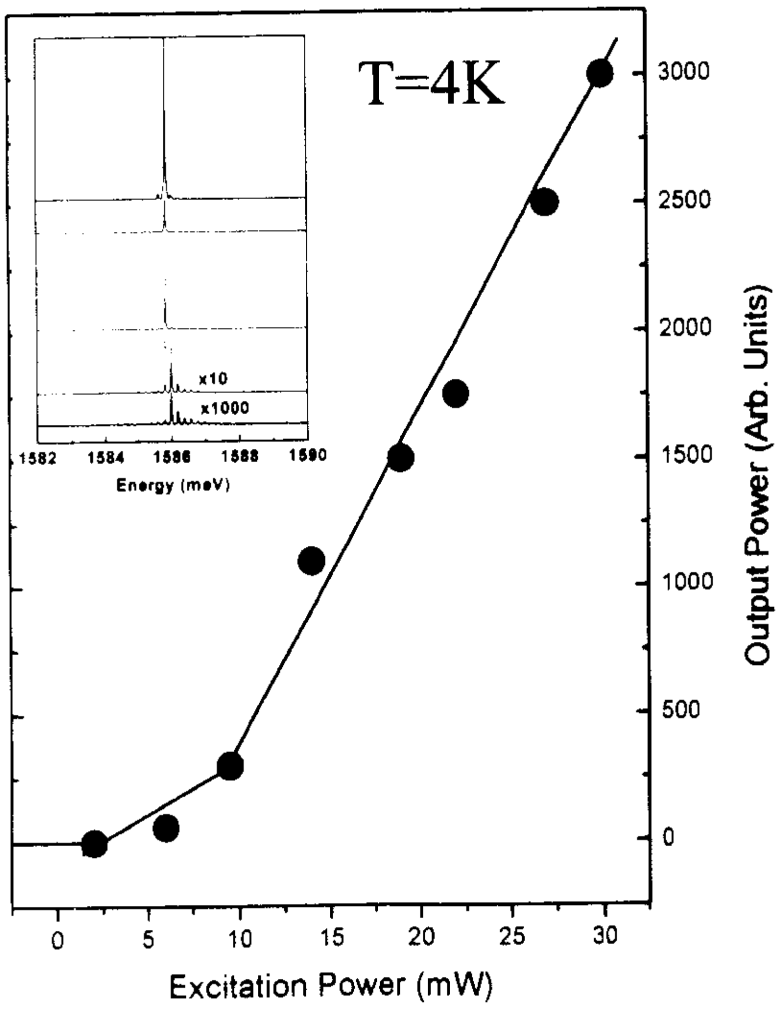

Experiment

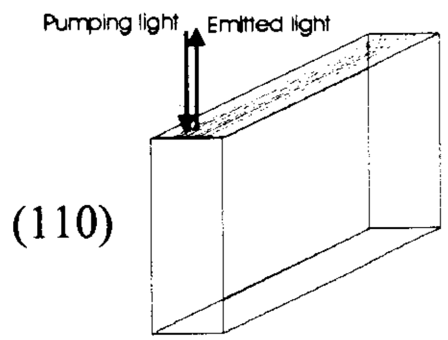

λ=736 nm
Objective NA=0.55

600μm cavity length with uncoated mirrows

pendence

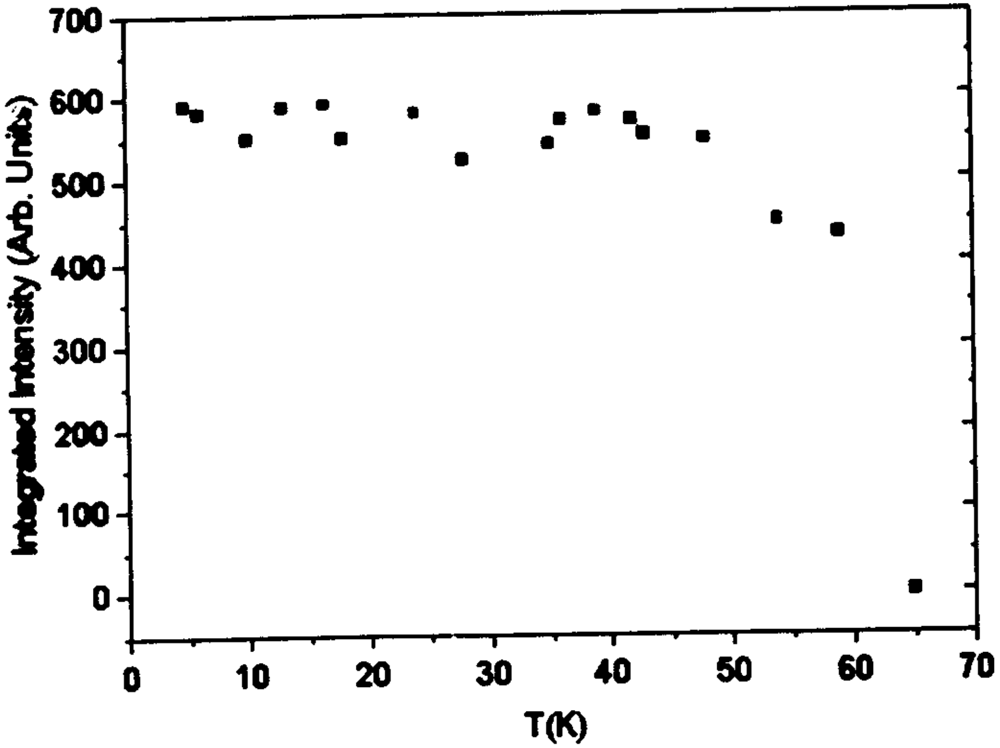

λ=736nm

Objective NA=0.55

600μm cavity length with
uncoated mirrows

INFM Current Injection QWR Laser

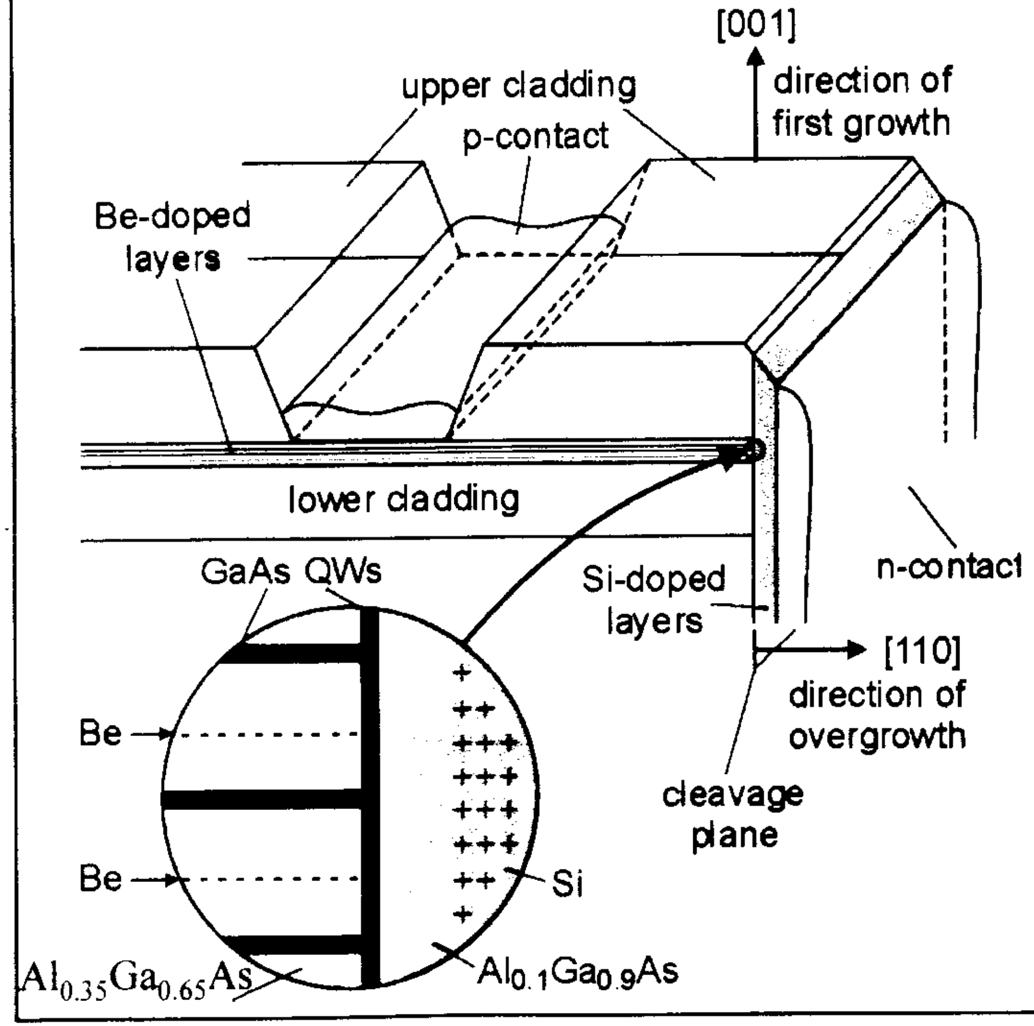

P-type contacts => evaporation of an AuBe layer on a partially etched upper cladding layer

n-type contacts => evaporation of a Ni/Ge/Au multilayer

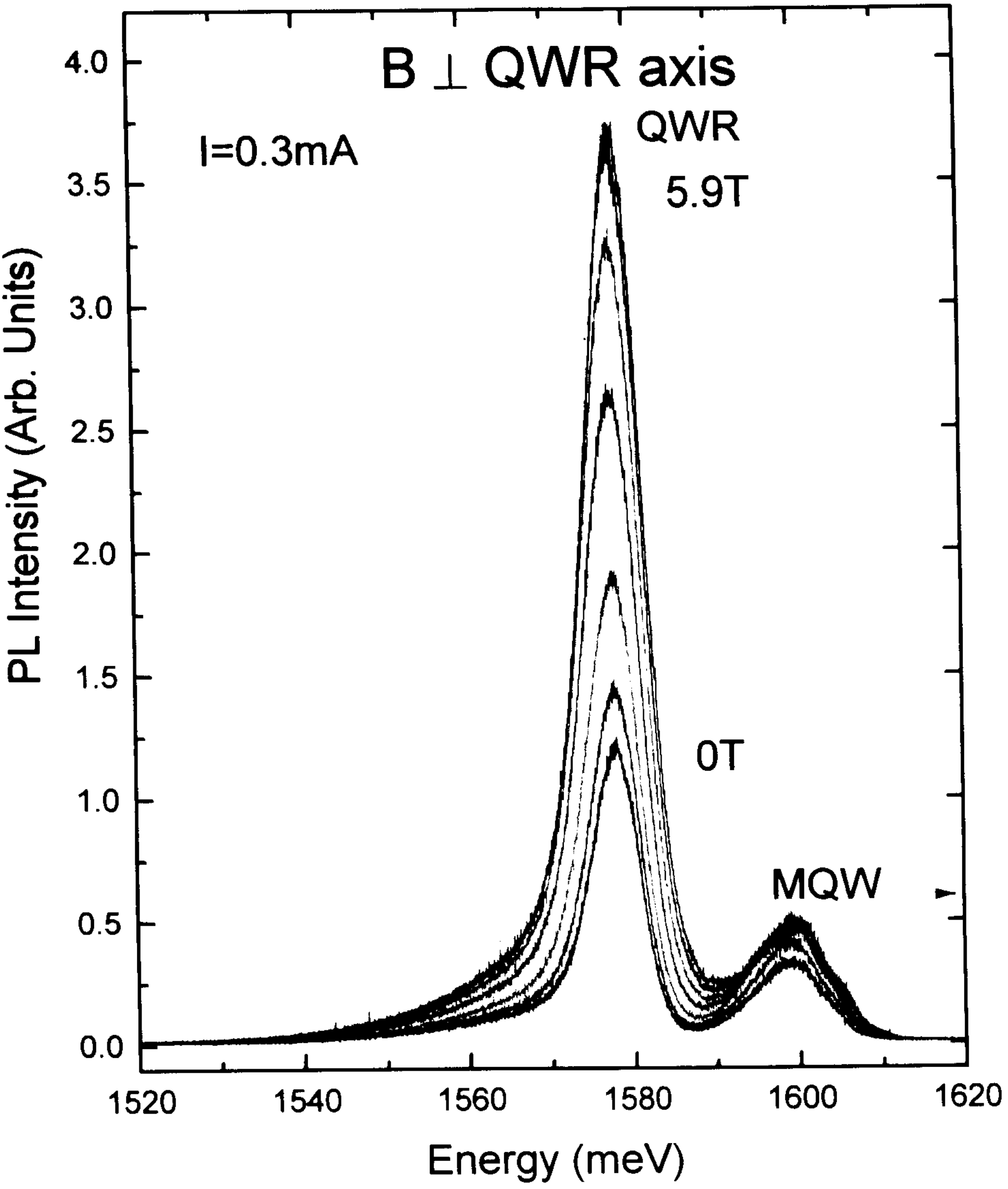
B ⊥ QWR axis
I=0.3mA
QWR
5.9T
0T
MQW
PL Intensity (Arb. Units)
0.0
0.5
1.0
1.5
2.0
2.5
3.0
3.5
4.0
Energy (meV)
1520
1540
1560
1580
1600
1620

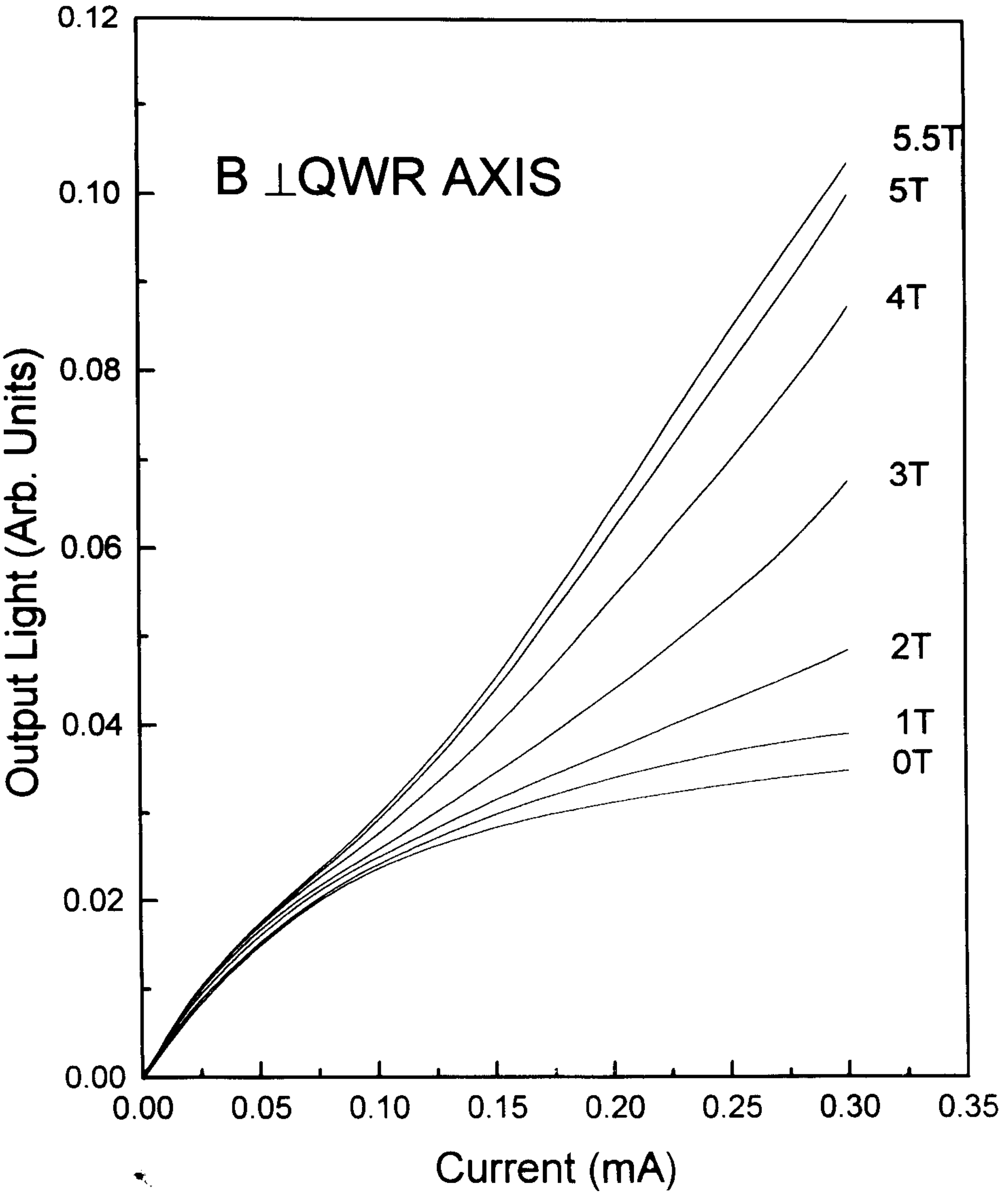

Saha et. al , J. of Crystal Growth 201/202, 505 (1999)

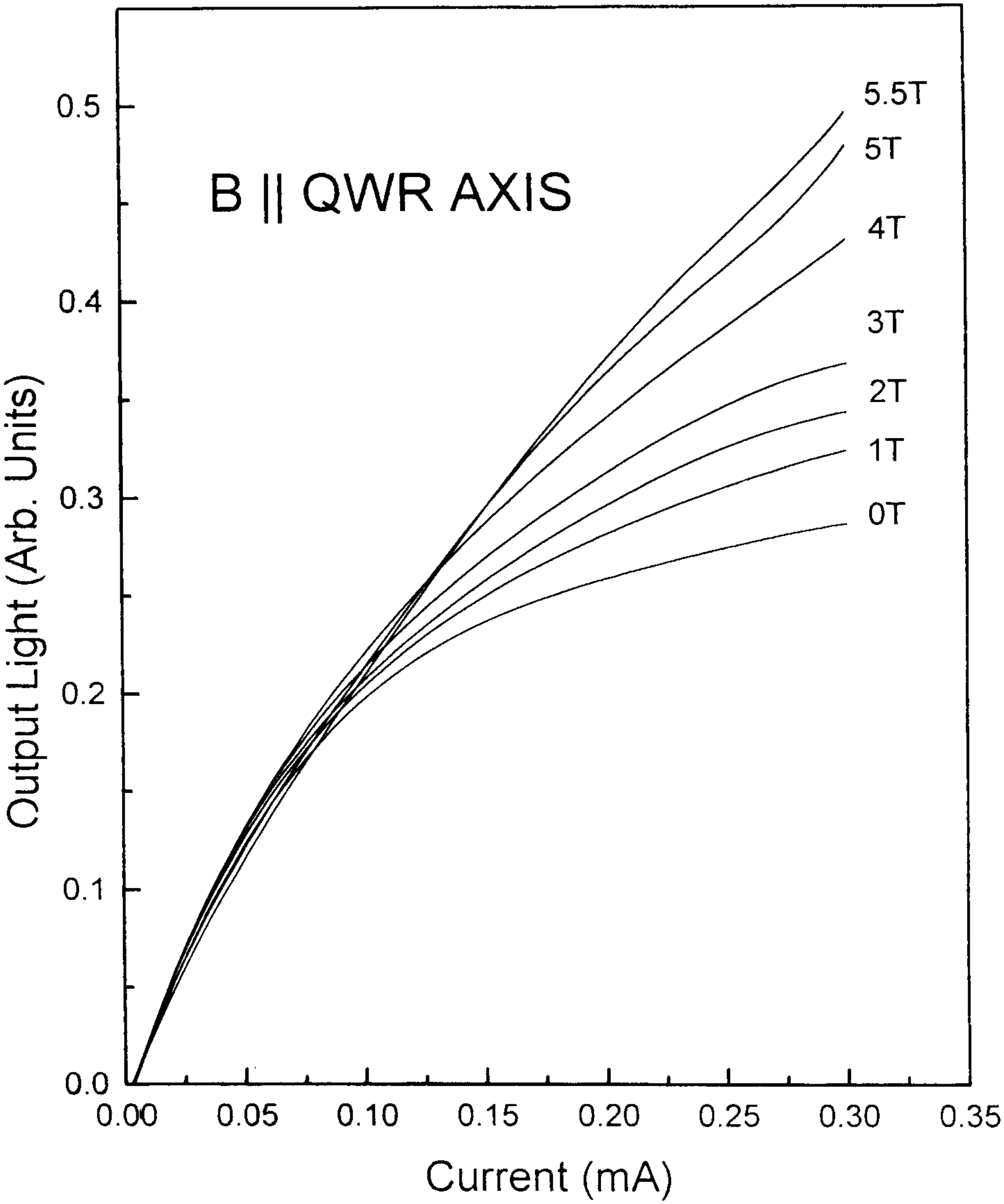
B || QWR AXIS
Output Light (Arb. Units)
0.0
0.1
0.2
0.3
0.4
0.5
Current (mA)
0.00
0.05
0.10
0.15
0.20
0.25
0.30
0.35
5.5T
5T
4T
3T
2T
1T
0T